Subsurface imaging of a nucleated cell based on two wrapped phase images

Yuanyuan Xu (徐媛媛)[1], Yawei Wang (王亚伟)[1,2*], Hui Wu (吴 慧)[2], Weifeng Jin (金卫凤)[1], Ying Ji (季 颖)[2], Min Bu (卜 敏)[2], and Li Zhang (张 力)[1]

[1]*School of Mechanical Engineering, Jiangsu University, Zhenjiang 212013, China*
[2]*Faculty of Science, Jiangsu University, Zhenjiang 212013, China*
[*]*Corresponding author: jszjwyw@sina.cn*

Received April 14, 2014; accepted July 16, 2014; posted online January 16, 2015

We present a simple method for the subsurface imaging of a nucleated cell, which is realized by measuring the difference in wrapped phase between a nucleated cell and its enucleated cell model. The latter one called as the reference phase can be simulated according to the axial thickness and the cytoplasmic refractive index. We illustrate the proposed method with theoretical analysis and numerical simulation of a binucleated cell, and prove its validity on real biological cells by imaging the HeLa cell based on its experimental phase. It shows that this method is suitable for imaging of relatively simple nucleated cells.

OCIS codes: 100.3008, 120.5050, 170.0180, 170.1530.
doi: 10.3788/COL201513.S11001.

Quantitative phase microscopy (QPM) allows the imaging of transparent biological specimen, such as live cells, without any exogenous contrast agents. So several QPM techniques have been proposed and successfully applied to explore the morphology and dynamics of biological cells[1–13], especially for the red blood cells (RBCs)[7–13]. The reason is that the mature RBC can be seen as a homogeneous object without nucleus, and its thickness information can be directly decoupled from the measured phase information. However, most biological cells are inhomogeneous, which contain nuclei and other intracellular organelles wherein the thickness and refractive index information are coupled into the phase information. Besides, their intracellular information, size, shape, volume, and surface roughness of organelles, such as the nucleus, are usually ignored. But this information is useful for medical diagnosis. For example, it is demonstrated that the shape and the roughness of the nucleus are closely related to cancer prognosis[14].

The phase signal depends on both the thickness and the refractive index of the specimen. In recent research, several methods have been proposed and successfully used for decoupling these two quantities. Among them, tomographic phase microscopy[15,16] is an effective one to get the three-dimensional refractive index. But, it refers to the mechanical scanning process and the reconstruct method of the refractive index is complicated. Using the QPM combined with confocal microscopy, which is needed for determining the physical height of a cell, the cellular integral refractive index along the axial direction can be computed[17,18]. Another common technique is acquiring twice quantitative phase images by utilizing surrounding media with slightly different refractive indices[19,20] or employing the dual-wavelength digital holographic microscopy[21], which can simultaneously decouple the axially averaged refractive index and physical thickness. However, the method of the subsurface information retrieval from the phase data has rarely been mentioned in each method. Based on this, Edward *et al.* presented a simple approach in which the quantitative phase and shear-force feedback topography data were simultaneously used to extract subsurface sample information[22]. Although this approach is very suitable for the imaging of individual cells, their experimental structures, including the optical setup and the electrical setup, are very complicated. In addition, the need of a custom-built near-field scanning optical microscope makes this method time-consuming.

In this letter, we present a simple method to extract cellular subsurface information on the basis of the difference in phases between a cell and its corresponding enucleated model. Among them, the phase of the enucleated model is approximately simulated by the axial thickness and the cytoplasmic refractive index. It is hereby demonstrated that this method is suitable for subsurface observation of nucleated cells through its application on a binucleated cell model and a HeLa cell.

Most live cells are phase objects, which do not absorb or scatter light significantly. The optical phase delay occurs when light traverses through them. Figure 1(a) shows the phase change of a simple cell with a nucleus induced on the transmitted wave. Assuming that the light propagates along the z-axis, the phase delay caused by the cell in the image plane (x, y) can be described as

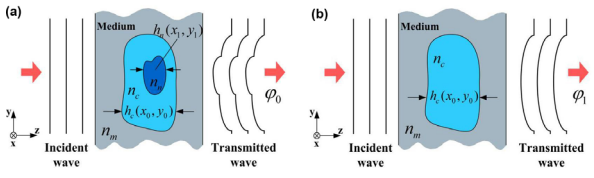

Fig. 1. Phase caused by a cell under a plane wave: (a) a nucleated cell and (b) enucleated cell model of (a).

$$\varphi_0(x,y)=\frac{2\pi}{\lambda}\left\{\int_0^{h_n(x,y)}[(n_n(x,y,z)-n_c(x,y,z)]\times \mathrm{d}z+\int_0^{h_c(x,y)}[n_c(x,y,z)-n_m]\times \mathrm{d}z\right\}, \quad (1)$$

where $n_n(x, y, z)$ and $n_c(x, y, z)$ are the refractive indices of the nucleus and the cytoplasm at points (x, y, z), respectively, n_m is the refractive index of the surrounding medium, $h_c(x, y)$ and $h_n(x, y)$ are the axial thicknesses of the cell and the nucleus, respectively.

The second term on the right side of Eq. (1) represents the phase delay caused by the refractive index difference between the cytoplasm and the surrounding medium along the axial thickness of the cell. It is regarded as the phase change of the cell without the nucleus, called as the reference phase (Fig. 1(b)). If the intracellular refractive index, n_c, is a constant, the reference phase can be simply written as

$$\varphi_1(x,y)=\frac{2\pi}{\lambda}(n_c-n_m)\times h_c(x,y). \quad (2)$$

Subtracting Eq. (2) from Eq. (1), one can obtain

$$\Delta\varphi(x,y)=\varphi_0(x,y)-\varphi_1(x,y)=\frac{2\pi}{\lambda}\int_0^{h_n(x,y)}[n_n(x,y,z)-n_c]\,\mathrm{d}z. \quad (3)$$

It can be seen from Eq. (3) that $\Delta\varphi(x, y)$ related to the nucleus is an integral of refractive index difference between the nucleus and cytoplasm. Once $\Delta\varphi(x, y)$ is calculated, the relative optical thickness of the nucleus, $\Delta S(x, y)$, can also be derived from it. That is

$$\Delta S(x,y)=\int_0^{h_n(x,y)}[n_n(x,y,z)-n_c]\mathrm{d}z=\frac{\lambda\Delta\varphi(x,y)}{2\pi}. \quad (4)$$

In order to further extract subsurface information, such as the morphology of the nucleus, for example, if the refractive index of the nucleus has been known as a constant n_n, the physical thickness of the nucleus $h_n(x, y)$ can be calculated, which is given by

$$h_n(x,y)=\frac{\lambda\Delta\varphi(x,y)}{2\pi(n_n-n_c)}=\frac{\lambda[\varphi_0(x,y)-\varphi_1(x,y)]}{2\pi(n_n-n_c)}. \quad (5)$$

It is easy to see that the acquisition of these two phase maps is a key task in the process of extracting subsurface information. Among them, the reference information, $\varphi_1(x, y)$, can be simulated according to the axial thickness and the cytoplasmic refractive index, wherein the axial thickness can be acquired in real experiments by applying a suitable technique, such as the confocal reflectance microscopy and dual-media quantitative measurement.

In general, the phase difference is measured based on the subtraction of two unwrapped phase maps. Here, we firstly measure the difference between two wrapped phases, then measure the corresponding unwrapped phase difference. More details are as follows.

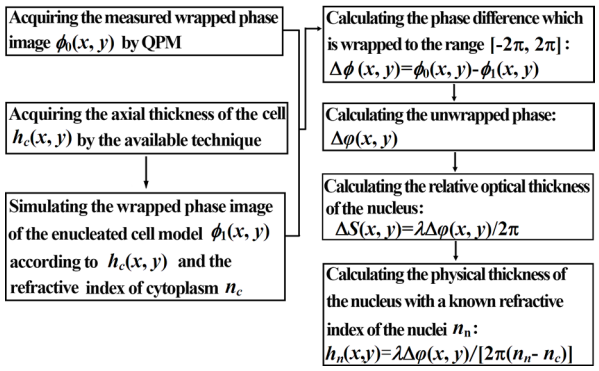

Fig. 2. Flow chart of subsurface imaging.

Assuming that $\phi_j(x, y)$ is the corresponding wrapped phase of $\phi_j(x, y)$, the following relationship is satisfied:

$$\varphi_j(x,y)=\phi_j(x,y)+2\pi k_j(x,y) \quad (j=0,1), \quad (6)$$

where $\phi_j(x, y)$ is wrapped to the range $[-\pi, \pi]$. k_j is an integer, but it is not a fixed constant. Thus $\varphi_j(x, y)$,is continuous, and Eq. (3) can be transformed to

$$\Delta\varphi=\varphi_0-\varphi_1=(\phi_0+2\pi k_0)-(\phi_1+2\pi k_1)=\Delta\phi+2\pi\Delta k, \quad (7)$$

where $\Delta\phi=\phi_0-\phi_1$, $\Delta k=k_0-k_1$. Note that $\Delta\phi$ represents the difference of two wrapped phases, which is wrapped to the range $[-2\pi, 2\pi]$.The phase difference $\Delta\varphi$ can be calculated via the corresponding unwrapping algorithm. Thus, we need less amount of calculation owing to which only one unwrapping operation is required. Figure 2 shows the flow chart of the proposed method for intracellular subsurface imaging.

To verify the reliability of this method, we firstly image a simulated binucleated cell. The whole cell model is shown in Fig. 3(a), where a sphere contains a small sphere and an ellipsoid, in which the radii of the ectosphere and the endosphere are set to be 6 and 2 μm, and the radii of the ellipsoid are 1, 1, and 3 μm along the x-, y-, and z-axes, respectively. In fact, the above model can be regarded as a simple approximate

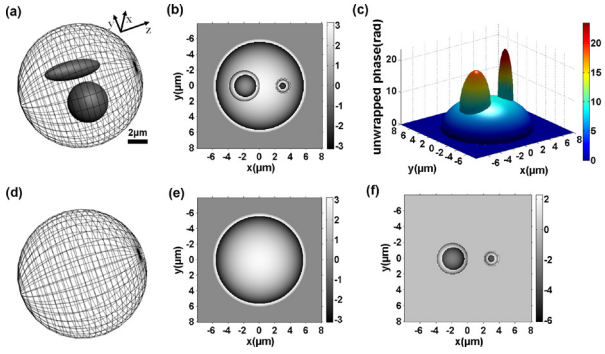

Fig. 3. (a) Spherical cell model with two nuclei, (b) wrapped phase image of (a), $\phi_0(x, y)$, (c) unwrapped phase image of (a), $\varphi_0(x, y)$, (d) spherical enucleated cell model, (e) wrapped phase image of (d), $\phi_1(x, y)$, and (f) wrapped phase difference between (b) and (e), $\Delta\phi(x, y)$.

model of the neutrophil or eosinophil by analyzing the morphology of white blood cells, in which the internal sphere and the ellipsoid are two nuclei of the cell.

In the simulations, the refractive indices of the nuclei, cytoplasm, and surrounding medium are set to be 1.6, 1.4, and 1.34, respectively, and the wavelength is 488 nm. The wrapped phase of the cell is obtained by simulation (Fig. 3(b)). The real phase is reconstructed by two-dimensional phase unwrapping (Fig. 3(c)). However, it cannot display the substructure of the cell accurately owing to which the cell is inhomogeneous resulting in a non-linear relationship between the phase and the thickness. Thus, both the useful thickness information and refractive index are coupled and cannot be calculated directly from the phase information. For this reason, the measurement of the reference phase information is necessary to decouple the inner components according to the above theory. Therefore, we build an enucleated cell model with its radius being 6 μm (Fig. 3(d)). The intracellular refractive index is the same as that of cytoplasm. Figure 3(e) shows the wrapped phase map of the enucleated cell via the simulation.

Then, the intracellular subsurface imaging can be achieved based on two wrapped phases. Firstly, by subtracting Fig. 3(e) from Fig. 3(b), we can compute the wrapped phase difference with value ranges from -2π to 2π (Fig. 3(f)). Then, the phase difference related to the nucleus is reconstructed from Fig. 3(f) by an appropriate phase-unwrapping algorithm (Fig. 4(a)). Secondly, according to Eq. (4), the relative optical thickness of the nucleus is directly computed from Fig. 4(a), which is shown in Fig. 4(b). Compared with Fig. 3(c), Fig. 4(b) displays the cellular subsurface information more clearly, which eliminates the annoyance to the observation of the substructure caused by the surface phase and optical thickness information. Thirdly, Fig. 4(c) shows the physical thicknesses of the nuclei $h_n(x, y)$, which is obtained by substituting the refractive index of the nuclei $n_n = 1.6$ into Eq. (5). In order to further demonstrate the correctness of our method and its

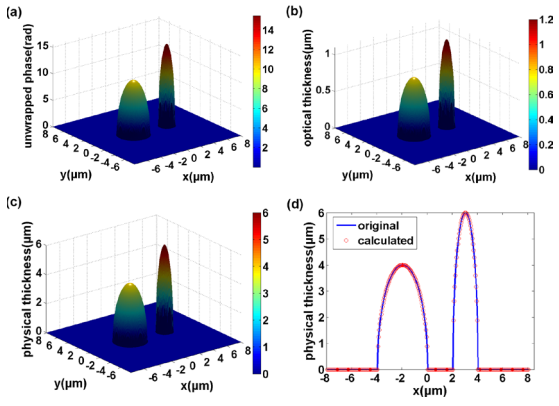

Fig. 4. (a) Unwrapped relative phase of the nucleus, $\Delta\varphi(x, y)$, (b) relative optical thickness of the nucleus, $\Delta S(x, y)$, (c) physical thickness of the nucleus, $h_n(x, y)$, and (d) central horizontal sections of the original and calculated thickness of the nucleus.

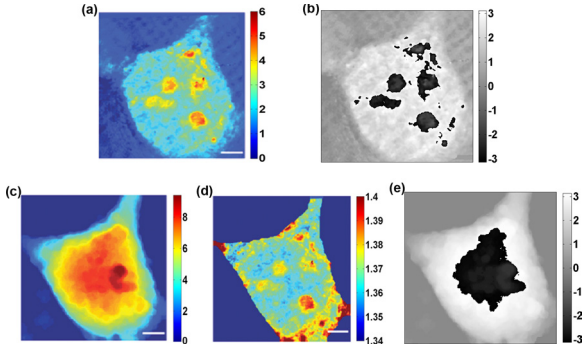

Fig. 5. HeLa cell: (a) phase image[17], (b) wrapped phase result of (a) $\phi_0(x, y)$, (c) thickness image[17], (d) axially averaged refractive index[17], and (e) wrapped phase image in the case of the enucleated cell model $\phi_1(x, y)$.

accuracy, the horizontal central sections of the original (set in the simulation) and the calculated physical thickness of the nucleus are set (Fig. 4(d)). These two curves are almost superimposed.

Furthermore, in order to demonstrate the method for the subsurface observation of real biological cells, we extracted the subsurface features of a HeLa cell. Similarly, it is necessary to obtain the corresponding wrapped phase maps of the HeLa cell and its equivalent enucleated cell model. Figure 5(a) shows the quantitative phase distribution of the HeLa cell measured by Lue *et al.* using Hilbert phase microscopy[17], and its wrapped result is shown in Fig. 5(b), which is measured by the add-wrapping algorithm. In general, the wrapped phase result is acquired before the unwrapped one in real quantitative phase imaging. To obtain the wrapped phase information of the equivalent enucleated HeLa cell, we need to know its axial thickness information and cytoplasmic refractive index, which have been measured by Lue *et al.*[17]. Among them, Fig. 5(c) shows the thickness distribution measured by confocal reflectance microscopy, Fig. 5(d) shows the axially averaged refractive index, in which the measured refractive index of cytoplasm is 1.375 ± 0.011[17]. Here, in order to simplify the calculation, we assume that the cytoplasmic refractive index is a constant of 1.375, which is regarded as the intracellular refractive index of the enucleated cell. In addition, the refractive index of surrounding medium is set to be 1.34, and the wavelength of the plane wave is 488 nm, both of which are same as the experimental value. Then, according to Eq. (3), the wrapped phase image can be simulated (Fig. 5(e)).

As the measured phase $\phi_0(x, y)$ (Fig. 5(a)) and the reference phase $\phi_1(x, y)$ (Fig. 5(e)) are known, we can successively extract the following results according to the flow chart (Fig. 2). Among them, Figs. 6(a) and (b) are the wrapped phase difference $\Delta\phi(x, y)$ with a larger range of $[-2\pi, 2\pi]$ and the unwrapped one $\Delta\varphi(x, y)$, respectively. Figure 6(c) shows the subsurface relative optical thickness $\Delta S(x, y)$. It can be seen from Figs. 6(b) and (c) that the intracellular information is displayed clearly, especially, the heave parts (red parts), which

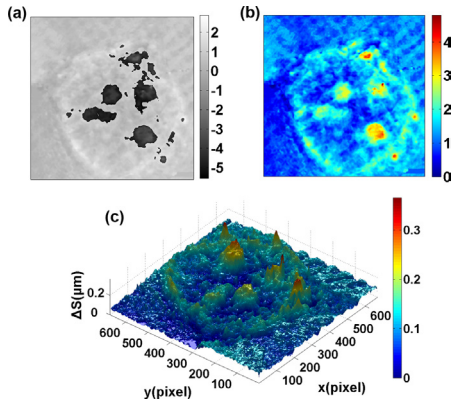

Fig. 6. (a) Wrapped phase difference, $\Delta\phi(x, y)$, (b) unwrapped result of (a), $\Delta\varphi(x, y)$, and (c) relative optical thickness of the substructure, $\Delta S(x, y)$.

correspond to the nucleoli of the HeLa cell owing to which they possess high refractive index than the rest of the cells. This result agrees well with the experimental result of Lue *et al.*[17]. It shows that the proposed method is applicable to subsurface imaging of real biological cells.

In conclusion, we present a simple effective method for intracellular subsurface imaging. By measuring two wrapped phase distributions of the cell and the enucleated model of the same cell, and calculating the difference between them, one can extract the relative phase and the optical thickness information, even the physical thicknesses of the nuclei with the known nuclear refractive index. A simulated binucleated cell and a HeLa cell are studied for demonstrating the reliability and ability of this method. The results show that the subsurface information related to the nuclei can be decoupled well. This method is better suitable for relatively simple cells imaging, because it is not entirely accurate in the process of obtaining the reference phase information when the cytoplasmic refractive index replaces the intracellular refractive index under the model of the enucleated cell, especially for some inhomogeneous objects with complex structures.

This work was supported by the National Natural Science Foundation of China (Nos. 11374130 and 11302086), the Doctoral Program Joint Fund of Colleges and Universities Specialized Research (No. 20113227110018), the Research Foundation for Advanced Talents of Jiangsu University (No. 12JDG059), the Jiangsu Postdoctoral Science Foundation (No. 1302094B), and the Innovation Program for College Graduates of Jiangsu Province (NO. KYLX_1017).

References

1. C. L. Curl, C. J. Bellair, P. J. Harris, B. E. Allman, A. Roberts, K. A. Nugent, and L. M. D. Delbridge, Clin. Exp. Pharmacol. Physiol. **31**, 896 (2004).
2. K. J. Chalut, W. J. Brown, and A. Wax, Opt. Express **15**, 3047 (2007).
3. B. Bhaduri, H. Pham, M. Mir, and G. Popescu, Opt. Lett. **37**, 1094 (2012).
4. Z. Wang, L. Millet, M. Mir, H. F. Ding, S. Unarunotai, J. Rogers, M. U. Gillette, and G. Popescu, Opt. Express **19**, 1016 (2011).
5. B. Kemper, A. Vollmer, C. E. Rommel, J. Schnekenburger, and G. V. Bally, J. Biomed. Opt. **16**, 026014 (2011).
6. M. Paturzo, A. Finizio, P. Memolo, R. Puqlisi, D. Balduzzi, A. Gall, and P. Ferraro, Lab Chip **12**, 3073 (2012).
7. B. Bhaduri, K. Tangella, and G. Popescu, Biomed. Opt. Express **4**, 1434 (2013).
8. G. Popescu, Y. K. Park, W. Choi, R. R. Dasari, M. S. Feld, and K. Badizadegan, Blood Cells Mol. Dis. **41**, 10 (2008).
9. Y. K. Park, M. Diez-Silva, G. Popescu, G. Lykotrafitis, W. Choi, M. S. Feld, and S. Suresh, Proc. Natl Acad. Sci. USA **105**, 13730 (2008).
10. Y. K. Park, C. A. Best, K. Badizadegan, R. R. Dasari, M. S. Feld, T. Kuriabova, M. L. Henle, A. J. Levine, and G. Popescu, Proc. Natl Acad. Sci. USA **107**, 6731 (2010).
11. G. Popescu, T. Ikeda, R. R. Dasari, and M. S. Feld, Opt. Lett. **31**, 775 (2006).
12. H. V. Pham, B. Bhaduri, K. Tangella, C. Best-Popescu, and G. Popescu, PLoS One **8**, e55676 (2013).
13. B. Rappaz, A. Barbul, A. Hoffmann, D. Boss, R. Korenstein, C. Depeursinge, P. J. Magistretti, and P. Marquet, Blood Cells Mol. Dis. **42**, 228 (2009).
14. H. W. Wolberg, W. N. Street, and O. L. Mangasarian, Clin. Cancer Res. **5**, 3542 (1999).
15. B. Simon, M. Debailleul, V. Georges, V. Lauer, and O. Haeberle, Eur. Phys. J. Appl. Phys. **44**, 29 (2008).
16. W. Choi, C. F. Yen, K. Badizadegan, S. Oh, N. Lue, R. R. Dasari, and M. S. Feld, Nat. Methods **4**, 717 (2007).
17. N. Lue, W. Choi, G. Popescu, Z. Yaqoob, K. Badizadegan, R. R. Dasari, and M. S. Feld, J. Phys. Chem. A **113**, 13327 (2009).
18. C. L. Curl, C. J. Bellair, T. Harris, B. E. Allman, P. J. Harris, A. G. Stewart, A. Roberts, K. A. Nugent, and L. M. D. Delbridge, Cytometry Part A **65A**, 88 (2005).
19. B. Rappaz, A. Barbul, Y. Emery, R. Korenstein, C. Depeursinge, P. Magistretti, and P. Marquet, Cytometry Part A **73A**, 895 (2008).
20. B. Rappaz, P. Marquet, E. Cuche, Y. Emery, C. Depeursinge, and P. J. Magistretti, Opt. Express **13**, 9361 (2005).
21. B. Rappaz, F. Charrière, C. Depeursinge, P. J. Magistretti, and P. Marquet, Opt. Lett. **33**, 744 (2008).
22. K. Edward, F. Farahi, and R. Hocken, Opt. Express **17**, 18408 (2009).